# Optimal Apodization Design for Medical Ultrasound using Constrained Least Squares. Part I: Theory

**D. A. Guenther and W. F. Walker**

## Abstract

Aperture weighting functions are critical design parameters in the development of ultrasound systems because beam characteristics affect the contrast and point resolution of the final output image. In previous work by our group, we developed a metric which quantifies a broadband imaging system's contrast resolution performance [1]. We now utilize this metric to formulate a novel general ultrasound beamformer design method. In our algorithm we use constrained least squares (CLS) techniques and a linear algebra formulation to describe the system point spread function (psf) as a function of the aperture weightings. In one approach we minimize the energy of the psf outside a certain boundary and impose a linear constraint on the aperture weights. In a second approach we minimize the energy of the psf outside a certain boundary while imposing a quadratic constraint on the energy of the psf inside the boundary. We present detailed analysis for an arbitrary ultrasound imaging system and discuss several possible applications of the CLS techniques, such as designing aperture weightings to optimize cystic resolution and improve the system depth of field. Simulation results are presented in an accompanying paper [2].

## Introduction

The determination of array aperture weights which produce a synthesized beam pattern with a narrow mainlobe and low sidelobes is a classical problem with a rich history in the signal processing literature. Dolph used Chebyshev polynomials to calculate aperture weights for a uniformly spaced, continuous wave linear array that achieved the minimum possible beamwidth

for a given maximum sidelobe level [3]. Taylor expanded this formulation to achieve tapered sidelobes further away from the mainlobe for continuous apertures [4], and Villeneuve applied it to discrete arrays [5]. Alfred H. Nuttall, in his paper [6], improved upon the Blackman-Harris window to achieve beam patterns whose maximum sidelobes are minimized. Whereas these previous papers focused on uniformly spaced arrays, Olen and Compton developed an iterative procedure using an arbitrarily shaped adaptive array to produce the desired sidelobe behavior by using a recursive feedback procedure [7]. Tseng and Griffiths also produced a simple iterative algorithm that can be used to find array weights for nonuniform geometries to produce beam patterns with a given look direction and minimum energy in the sidelobes [8]. An interesting outcome of their methods allowed for the design of beam patterns where the desired sidelobe response could vary with angle.

Although these previous methods produced excellent results narrowband assumptions, computational complexities, and iterative procedures limit their applicability to general ultrasound beamformer design. Considerable gains can be made in computation time with the use of least squares methods. In fact, over the last two decades many authors have developed constrained least squares algorithms for the design of FIR filters [9-12]. These methods typically minimize the error of the filter over a certain frequency band with respect to some desired filter response. For example, Selesnick described a constrained least squares approach to design FIR filters that did not require the specification of a transition band of frequencies between the passband and stopband. By setting up a minimization problem on the $l^2$ error of the filter's amplitude response subject to linear equality constraints, Selesnick derived filters with minimum error and devoid of Gibb's phenomenon [9]. Other authors used least squares methods to produce eigenfilters, or filters that minimize a quadratic error measure in the passband and

stopband [10-12]. Later in a series of papers, Er *et al.* employed a variety of constrained least squares techniques to synthesize arbitrary array patterns subject to different criteria such as sidelobe level and mean squared sidelobe energy. Their algorithms employ linear and quadratic constraints to achieve array patterns for general array geometries which produce beam patterns that are highly directional with very low sidelobes [13-18].

The rich history of array pattern synthesis optimization has been only recently applied to medical ultrasound imaging and most applications have been specialized [19-23]. For example, Ebbini and Cain [19] proposed a method for synthesizing multiple focal regions on single transmit events for applications in hyperthermia treatment via ultrasound. Li *et al*. [20] used a total least squares method to compensate for psf degradation due to "dead" array elements or elements blocked by acoustically opaque windows in the interrogated media. Recently, Wilkening *et al.* designed optimal FIR filters for improved image contrast in contrast agent imaging [22] and FIR filters that increased the depth of field for dynamic receive focusing [23]. Although insightful and useful, these methods failed to address the larger problem of general beam pattern synthesis given arbitrary arrays. Previously, our group developed a general aperture design tool, supported by rigorous theory that is applied to the design of aperture weighting functions for arbitrary system design [24], [25]. The method utilized a minimum sum squared error (MSSE) formulation between the system psf and the desired or goal psf. One strength of the approach is that it allowed for full beam optimization given system parameters obtained through theory, simulation, or experiment. The method is useful because it allows for the design of any controllable system parameter in a straightforward, rigorous, time efficient manner. Ranganathan's approach, although extremely useful in aiding the design of prototype systems, suffers from the lack of a quantitative measure detailing how system performance

changes with respect to a deviation in system parameters. Furthermore, the approach offers no guidance in the selection of an appropriate goal point spread function. These shortcomings make system optimization using the MSSE approach difficult.

The method of apodization profile design presented in this paper is general enough to be applied to any coherent imaging system and is similar to many of the previous array pattern synthesis techniques utilizing constrained least squares (CLS). For example, our linearly constrained least squares (LCLS) formulation is similar to the array pattern synthesis technique by Tseng [8], and our quadratically constrained least squares (QCLS) formulation is similar to the constrained eigenfilter design [10], [26]. However while these prior analyses were for a single carrier frequency, we use a broadband formulation. Keitmann-Curdes *et al.* [27] previously developed an algorithm similar to our QCLS formulation which generated apodization profiles for ultrasound imaging with minimum sidelobe energy of the two dimensional space-time psf. Recently Schwann *et al.* used two different resolution criteria to design optimal frequency dependent apodization profiles [28], a method whose goals are similar to ours of improving image contrast. However, their multiple objective formulation requires computationally expensive iterative methods to arrive at one Pareto optimum solution, or a solution where further improving one objective necessarily degrades all others [29]. Further review of the differences between our LCLS and QCLS methods and the techniques mentioned above will be discussed in more detail later in this manuscript.

Since the ultrasound system's beam characteristics fundamentally affect the quality of the image, a great deal of effort is put into optimizing system parameters. Estimating the imaging performance of ultrasound systems is critical, both to characterize the fundamental imaging limits of the system, and to optimize image quality. It is possible to estimate the performance of

existing systems by imaging phantoms or human subjects, but it is necessary during system design to be able to determine imaging performance prior to system construction. The ability to accurately predict performance enables system optimization, quantitative consideration of engineering tradeoffs, and significantly reduces the time and cost investment in system development.

Synthesis of beampatterns in diagnostic ultrasound receives a great deal of attention during system design. The system's spatial impulse response, or point spread function, characteristics will determine such parameters as point resolution and contrast in the resulting image. Thus control over mainlobe width and sidelobe level is significant. These beam parameters are influenced by the size of the active aperture, the frequency of the ultrasound pulse, the magnitude and phase (or time delay) of the weightings applied to the active elements, and the pulse length. Because so many factors affect the characteristics of the psf and there is no global parameter describing psf quality, beamforming parameters are usually determined through iterative simulation and experimentation.

A quantitative resolution metric is essential to guide optimization of system parameters, including the system's psf. The most common measure of scanner performance is the beamplot [30], which has been adapted from RADAR. The -6dB beamwidth of the beamplot, the full width at half maximum (FWHM), and the beamwidth at other levels are used to estimate scanner resolution. Sidelobe and grating lobe levels are used to estimate eventual image contrast. Although widely used in medical ultrasound, there are scenarios in which the FWHM criterion indicates excellent performance, but actual images of tissue do not reveal important details.

Vilkomerson *et al.* addressed the limitations of the beamplot and proposed the concept of "cystic resolution" [31] in which performance was quantified as the size of a void that produced

a given contrast. The analysis, while novel and useful, was limited to narrowband circular apertures and neglected the axial dimension. Johnson [32] further developed the contrast resolution metric to include a 3D broadband model for circular apertures and compared different imaging parameters using maximum output contrast curves versus cyst diameter. Üstüner *et al.* [33] extended cystic resolution to a 3D broadband model for arbitrary apertures, but did not describe its theoretical foundation, resulting in a limited understanding of the formulation and its utility and drawbacks. A general cystic resolution metric was previously derived by our group [1]. This metric accounts for the effect of electronic noise and, under certain assumptions, reduces to that described in [33]. Whereas, the FWHM criterion sometimes provides misleading information about resolution in ultrasound systems, the cystic resolution metric identifies specific points in the psf of the system that can be optimized to increase image quality and performance.

This paper utilizes the cystic resolution metric to guide optimization of apodization profiles for coherent imaging systems. Specifically, we design optimal receive apodization profiles for a 1D linear array; however, our theory can be applied to a 2D array of arbitrary geometry and can be used to design one way or two way apodization profiles. We propose two different methods for optimal apodization design. The first algorithm minimizes the energy of the psf outside some specified region subject to a linear constraint of the apodization weights. We call the resultant weights the linearly constrained least squares (LCLS) apodization profile. The second algorithm minimizes the energy of the psf outside some region subject to a quadratic energy constraint of the psf inside the boundary. We call the resultant weights the quadractically constrained least squares (QCLS) apodization profile.

Our CLS apodization design methods return real weights and achieve a spatial impulse response with minimum sidelobe levels in a least squares sense given a specified mainlobe area. We formulate the problem starting from basic principles of acoustic wave diffraction theory and apply linear algebra techniques to represent the system psf. We generate a least squares problem subject to either a linear or quadratic constraint in order to minimize the energy outside a given mainlobe area in the psf. The algorithm can be applied to enhance the depth of field (DOF) in an imaging system as well as improve lesion detectability in inhomogeneous scattering media. The algorithm is arguably optimal for detecting anechoic cysts via ultrasound; however we believe it will also improve ultrasound system performance in general imaging applications. This paper outlines the theoretical description of the constrained least squares technique for designing apodization profiles for broadband, coherent imaging systems, describes a technique for reduced computational cost, and finally discusses examples of application. Results from simulations are presented in an accompanying paper [2].

## Theory

We present two-way broadband formulations for the LCLS and QCLS apodization design technique. The one-way broadband formulation can be expressed in a similar manner; however we note that in most ultrasonic imaging applications, apodization is typically applied only on receive and the two-way impulse response is of greater interest.

### *Linear Algebra Formulation of the Broadband Spatial Impulse Response (psf)*

The acoustic pressure field emanating from a transducer during pulse echo propagation at a single point in space at a single instant in time can be expressed as the product of a propagation

matrix, *S*, and a set of aperture weightings, *w*. The propagation matrix uses superposition to describe the contribution of each transducer element at each field point at an instant in time. The propagation function may be derived from the Rayleigh-Sommerfeld diffraction equation derived in ([34, pp.46-50]) and may also include a term relating to limited element angular response [35]. Alternatively, the propagation matrix may be computed via broadband simulation or estimated experimentally. For our formulation, *S* is a function of the transmit aperture weights, the excitation pulse, and the individual element impulse responses of the transmit and receive apertures [24].

The two way pulse echo propagation matrix, *S*, for a fixed transmit aperture and a *n* element receive aperture at a total number of *p* points in three dimensional space is:

$$S = \begin{bmatrix} s_{1,1} & s_{1,2} & \cdots & s_{1,n} \\ s_{2,1} & . & \cdots & . \\ \vdots & \vdots & \ddots & \vdots \\ s_{p,1} & . & \cdots & s_{p,n} \end{bmatrix}, \tag{1}$$

where $s_{i,j}$ is the contribution of the *j*th element at the *i*th point in space. The receive aperture weighting function, $w$ , for each of the *n* elements used on receive can be written in vector form as:

$$w = \begin{bmatrix} w_1 & w_2 & w_3 & \cdots & w_n \end{bmatrix}^T, \tag{2}$$

where T denotes the vector transpose operation. Using (1) and (2), we can now write the complete two-way pulse echo system psf, $P$, as follows:

$$P = Sw, \tag{3}$$

the propagation matrix multiplied by the receive weighting vector. Note that this results in the one dimensional column vector, $P$, of length $p$ the total number of points in three dimensional space where the system psf is measured.

This formulation can be expanded to describe the psf as a function of time. In this case, the receive weightings would be a function of element number and time, essentially forming the coefficients of a FIR filter on each receive channel. Adequate spatial and temporal sampling of the three dimensional psf yields huge propagation matrices, and therefore for this and the accompanying paper we have limited our analysis to a single instant in time and two spatial dimensions, azimuth and range. Clearly the elevation dimension matters in planar ultrasonic B-mode images, even with acoustic lenses on linear arrays. However, restricting our analysis to two dimensions eases visualization of the algorithm while still providing meaningful results.

*Cystic Resolution Metric*

The goal of the cystic resolution metric is to quantify the contrast resolution of an arbitrary broadband ultrasound system. We refer the reader to [1] for a more detailed discussion of the derivation of the metric and highlight the meaningful results here. The metric completely characterizes the 4D spatiotemporal contrast performance for a system imaging an anechoic void. However, analysis at the instant in time when the received signal is minimum (i.e. when as much of the psf energy as possible lies within the cyst) is usually sufficient. At this single instant in time, the psf can be expressed as a function of 3D space at the time of interest. The SNR is also considered at the time of interest ($SNR_{t_o}$). The contrast of the cyst relative to the background is defined as the ratio of the rms signal received from the cyst to the rms signal received from the background [1]:

$$C_{t_0} = \sqrt{\frac{1 + SNR_{t_o}^2 \frac{E_{out}}{E_{tot}}}{1 + SNR_{t_o}^2}} \quad , \tag{4}$$

where $E_{out}$ is the psf energy outside the cyst and $E_{tot}$ is the total psf energy, both at time $t_o$. Equation (4) describes the contrast of an anechoic cyst, whose size and location are described by a mask, relative to background speckle obtained by an imaging system with a given psf and electronic SNR defined statistically by $SNR_{t_o}$. Neglecting electronic noise, $SNR_{t_o}$ becomes infinite and (4) can be modified to the equation for contrast presented in [33], which is simply the square root of the ratio of the psf energy outside the cyst and the total psf energy:

$$C_{t_o} = \sqrt{\frac{E_{out}}{E_{tot}}} \quad . \tag{5}$$

The contrast for cysts of different sizes can be computed using the above expressions for cystic contrast, and system performance can be characterized as a function of cyst size as in [1, 31-33]. This metric can be used for 4D spatiotemporal analysis of broadband ultrasound systems, but 3D spatial analysis using (4) or (5) is typically adequate to characterize scanner performance as temporal analysis does not usually provide critical information. Note that in certain cases, it is valuable to compute the metric with cysts at different locations to quantify the depth of field, the effect of dynamic focusing, and other factors pertaining to the shift variance of the imaging system. Note also that while the metric can be used to determine cystic resolution, it can also be used to optimize system parameters by computing contrast as a function of cyst size and determining parameter values that maximize the contrast at the cyst sizes of interest.

*Linearly Constrained Least Squares (LCLS) Apodization Design*

One conspicuous result of the above resolution metric is that cystic contrast, or our objective function, is defined in terms of the spatiotemporal psf energy. In fact, contrast would be maximum if all the energy of the psf lay inside the void of the cyst. Whereas beamplot details can be misleading about overall image quality, this metric considers the psf globally to determine the impact on cystic contrast. Contrast improves when the psf energy outside the cyst boundary is reduced or the psf energy inside the cyst is increased. The cystic resolution metric defines a simple objective function for maximizing cystic contrast. The reader should note that different objective functions could be formulated, such as improving point contrast, but for the discussion presented here we focus on improving cystic contrast.

Cystic contrast is degraded by the presence of psf energy outside the cyst. We minimize this energy by solving for the set of receive aperture weights that, when applied to the synthetic receive element responses, will yield a psf with minimum energy outside the designated cyst boundary. Combining the above resolution metric with our linear algebra formulation of the psf, our beam synthesis problem becomes determining the vector of weights that minimize the psf energy outside the cyst boundary subject to a linear constraint to avoid the trivial case of all the receive weights set equal to zero. This is analogous to the problem of solving for the set of FIR filter coefficients that minimize the energy in the stopband.

Assuming the psf is focused at the center of the cyst, the algorithm is initialized by selecting the spatial points of the psf which lie outside the cyst boundary. We form the associated propagation matrix, $S$, which has as many rows as the number of points outside the cyst region and as many columns as elements in the active receive aperture. Therefore, each column of the $S$ matrix is one focused synthetic receive element response at all the spatial points outside the cyst boundary. Ranganathan's MSSE beamformer design approach outlined in [24]

and [25] uses focused or unfocused aperture propagation matrices. Although imaging scenarios exist with unfocused apertures, for the CLS apodization design technique presented here, we pre-focus our two way psfs so that the peak of the mainlobe lies in the center of the cyst boundary. This allows us to maximize the cost function in (5), cystic contrast. Using unfocused apertures is possible with the CLS formulation, but unfocused apertures would not typically be used for imaging cysts so a new cost function should be derived to reflect the system's intended application.

The CLS algorithm calculates the weights which minimize the energy in the sidelobe regions while simultaneously maintaining a peak gain at the center of the cyst. These weights are determined from the constrained least squares problem:

$$\min_{w} \left\| Sw \right\|^2 \quad \text{subject to the linear constraint} \quad C^T w = 1 \quad . \tag{6}$$

In this expression $\|\bullet\|^2$ denotes the square of the $\ell^2$-norm and the row vector $C^T$ has elements corresponding to the amplitude of each synthetic receive element response. More specifically, $C^T$ is a vector of the amplitudes of the receive element responses at the focus in the center of the cyst. The expression in (6) is common in the signal processing literature and drawing upon [36] the optimal receive aperture weightings are given by:

$$w_{opt} = (S^T S)^{-1} C [C^T (S^T S)^{-1} C]^{-1} \ , \tag{7}$$

where $(\bullet)^{-1}$ denotes the matrix inverse operation. Equation (7) provides a simple method to calculate the receive weightings that will minimize the energy in the psf outside a specified mainlobe region while simultaneously achieving peak gain inside the mainlobe region. The optimal receive weights minimize $E_{out}$ in (5) above, so we expect to see improved cystic contrast

using the LCLS apodization windows over commonly used windows such as the flat, Hamming and Nuttall [6] windows.

*Linearly Constrained Least Squares Apodization Design with Weighting Function*

In certain applications, the psf characteristics at specific spatial positions may be more important than others because of the effects that the psf has on point resolution and system contrast. For example, in hyperthermia applications the ultrasonic field pattern requires high power levels at some points while reducing the power deposition at other potential hot spots [19]. In other applications, it may be more important to reduce sidelobe levels than to precisely control the mainlobe. In these cases and others we can incorporate a weighting function, $g$, that emphasizes or deemphasizes certain spatial points in the psf during the apodization design procedure. The LCLS apodization design problem can be rewritten with the weighting function as:

$$\min_{w} \|g_d S w\|^2 \quad \text{subject to the linear constraint} \quad C^T w = 1 \ , \tag{8}$$

where $g_d$ is a diagonal $p$ x $p$ matrix with elements of $g$ along the 0th diagonal. The elements of $g$ have a large value where minimizing psf energy is important and smaller values where the psf energy is less critical. The solution for optimal receive weightings, drawing upon [36] is:

$$w_{opt} = (S^T g_d^T g_d S)^{-1} C [C^T (S^T g_d^T g_d S)^{-1} C]^{-1} \ . \tag{9}$$

*Quadratically Constrained Least Squares (QCLS) Apodization Design*

The LCLS apodization design algorithm minimized the energy in the psf outside a given region of the mainlobe. By doing so the cystic contrast should improve according to (5). This

analysis minimizes the numerator of (5); however, it ignores the denominator. As a result, although the energy outside the cyst will be minimized the total psf energy could also be decreased thus limiting cystic contrast improvements. We therefore develop an alternate approach where we minimize the energy of the psf outside a given boundary while at the same time keeping the energy of the psf inside the boundary constant. This formulation becomes similar to the earlier beam synthesis problem of creating eigenfilters [10], [26]. In the FIR eigenfilter design case, the energy constraint on the filter coefficients is usually just the quadratic constraint $w^T w = 1$ which constrains the total energy of the filter's frequency response to be unity. However, for broadband beamformers, this constraint is meaningless and we must devise a new formulation [26]. The modified quadratic constraint is straightforward given the cystic resolution metric. We wish to minimize $E_{out}$ while maximizing $E_{tot}$ in (5), and we can change $E_{tot}$ to just the psf energy inside the cyst boundary, $E_{in}$. Note that this problem can be set up as a multiple objective optimization problem [29], [37]. However, that approach does not yield an intuitive optimal solution like utilizing the cystic resolution metric does. Therefore, we choose to formulate this problem using a quadratically constrained least squares formulation:

$$\min_{w} \left\| S_{out} w \right\|^2 \quad \text{subject to the quadratic constraint } \left\| S_{in} w \right\|^2 = 1 \ , \tag{10}$$

where $\left\| \bullet \right\|^2$ denotes the square of the $\ell^2$-norm, $S_{out}$ is the propagation matrix for all the spatial points of the psf lying outside the cyst boundary, and $S_{in}$ is the propagation matrix for all the spatial points of the psf lying inside the cyst boundary. Note that the quadratic constraint essentially keeps the energy of the psf inside the cyst constant. Drawing upon [26], [38-40] the optimal receive aperture weightings satisfying the quadratic constraint is the generalized eigenvector, $w_{eig}$, corresponding to the minimum generalized eigenvalue resulting from the

generalized eigenvalue decomposition problem of $S_{out}^T S_{out}$ and $S_{in}^T S_{in}$. The generalized eigenvalue problem [38, pp. 375-376] for a matrix pair, ($A$, $B$) both n x n matrices, is finding the eigenvalues, $\lambda_k$, and the eigenvectors, $x_k \neq 0$, such that:

$$Ax_k = \lambda_k B x_k \quad . \tag{11}$$

The number of eigenvalues, $k$, is dependent upon the rank of matrix $B$. One of the main advantages of the QCLS technique is that no matrix inversion is required to solve for the optimal apodization profile, unlike the LCLS apodization design.

*Quadratically Constrained Least Squares Apodization Design with Weighting Function*

As with the LCLS apodization design, a weighting function, $g$, can be added that emphasizes or deemphasizes certain regions of the psf during the minimization process. Rewriting the QCLS apodization design problem above with the added weighting function we arrive at:

$$\min_w \left\| g_{out} S_{out} w \right\|^2 \quad \text{subject to the quadratic constraint } \left\| g_{in} S_{in} w \right\|^2 = 1 \ , \tag{12}$$

where $g_{out}$ is a diagonal $p$ x $p$ matrix with elements of $g$ associated with the spatial points of the psf outside the cyst boundary along the 0th diagonal, and $g_{in}$ is a diagonal $q$ x $q$ matrix with elements of $g$ associated with the spatial points of the psf inside the cyst boundary along the 0th diagonal. We solve this problem by forming the Lagrangian and utilizing the necessary conditions for a minimum:

$$L(w\ ,\lambda) = w^T S_{out}^T g_{out}^T g_{out} S_{out} w\ - \lambda(w^T S_{in}^T g_{in}^T g_{in} S_{in} w\ - 1)\ , \tag{13}$$

where λ is the associated Lagrange multiplier. Following the Kuhn-Tucker conditions, a necessary condition for a minimum is that $\frac{\partial L}{\partial w} = 0$ [37]. Thus taking the associated partial derivative of the Lagrangian with respect to the weighting vector we arrive at:

$$S_{out}^T g_{out}^T g_{out} S_{out} w\ = \lambda\, S_{in}^T g_{in}^T g_{in} S_{in} w\ . \tag{14}$$

Therefore the set of optimal receive weightings satisfying (14) is again the generalized eigenvector, $w_{eig}$, corresponding to the minimum generalized eigenvalue resulting from the generalized eigenvalue decomposition problem of $S_{out}^T g_{out}^T g_{out} S_{out}$ and $S_{in}^T g_{in}^T g_{in} S_{in}$.

*Reduced Computational Cost Through Symmetry Relations*

The computation of CLS apodization profiles requires significant resources due to the large propagation matrices and matrix inverse operations (for the LCLS design method). In order to reduce the computational complexity of the algorithm we take advantage of the lateral symmetry present in the system psf for symmetric, non-steered apertures. This symmetry means that we can use just half of the system psf for the calculations of the optimal weightings. The propagation matrix, *S*, then becomes:

$$S = \begin{bmatrix} s_{1,1} & s_{1,2} & \cdots & s_{1,n} \\ s_{2,1} & . & \cdots & . \\ \vdots & \vdots & \ddots & \vdots \\ s_{p/2,1} & . & \cdots & s_{p/2,n} \end{bmatrix}\ , \tag{15}$$

where $S$ is a ($p$/2) x ($n$) matrix, consisting of the pressure field at only $p$/2 points in space for each element [1, 2, … $n$].

The symmetry of the non-steered receive aperture is another property that can be exploited to reduce computational cost. As shown in Fig. 1, pairs of elements can be grouped together that are the same distance from the center axis of the array. Pairing is possible because these elements should have the same weights applied, assuming no beam steering and an even number of elements in the aperture. Therefore the propagation matrix can be rewritten:

$$S = \begin{bmatrix} s_{1,1,n} & s_{1,2,n-1} & \cdots & s_{1,n/2,n/2+1} \\ s_{2,1,n} & . & \cdots & . \\ \vdots & \vdots & \ddots & \vdots \\ s_{p/2,1,n} & . & \cdots & s_{p/2,n/2,n/2+1} \end{bmatrix}, \tag{16}$$

where $s_{i,j,k}$ is the response at the point $i$ in space for the element $j$ plus the response for element $k$ at the same point in space. The aperture weights must also be reshaped as:

$$w = \begin{bmatrix} w_{1,n} & w_{2,n-1} & w_{3,n-2} & \cdots & w_{n/2,n/2+1} \end{bmatrix}^T, \tag{17}$$

where $w_{i,j}$ is the weight applied for element $i$ and element $j$, respectively.

The derivation is now analogous to that in (6) and (10) and the optimal weights can be determined directly. The use of symmetry reduces the size of the propagation matrix, $S$, by a factor of 2 in each dimension, for a total reduction of a factor of 4 in memory requirements. The computational savings will be even greater since the necessary solution algorithms have polynomial costs as a function of matrix size.

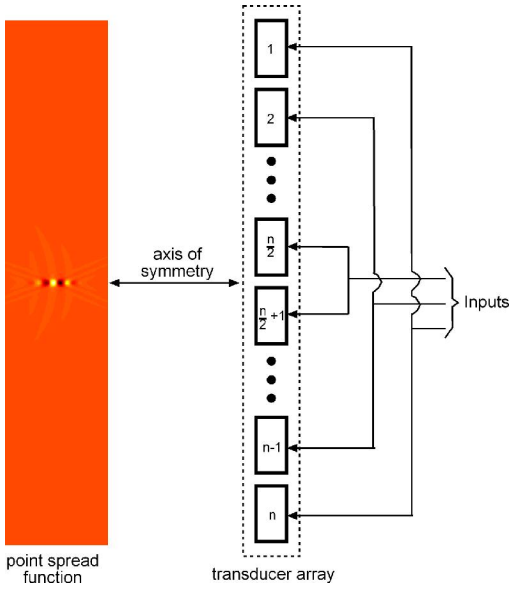


Fig. 1. Exploitation of symmetry for reduced computational cost. The aperture is symmetric about the center axis; therefore pairs of elements that would have the same weights are grouped together. Also, the lateral symmetry in the psf about the same center axis allows for analyzing just one half of the psf. This symmetry assumes a symmetric non-steered aperture.

## Applications

Although the CLS apodization profiles discussed above were constructed to optimize cystic resolution, the techniques are general enough to be applied in wide-ranging scenarios. A few possible applications are described.

### *A. Improved Cystic Contrast and Improved Point Resolution*

The cystic resolution metric described in [1] stated that the point contrast of an ultrasound system imaging a cyst is a function of the psf energy. Neglecting system SNR, we note that according to (5) we can improve the contrast of a cyst in two ways. If we minimize the energy of the psf outside the cyst boundary, the numerator in (5) decreases and contrast improves. Furthermore, if we minimize the energy of the psf outside the cyst boundary and increase the

energy of the psf inside the cyst boundary, contrast will improve even more dramatically. The LCLS and QCLS methods described above minimize the psf energy outside a specified boundary subject to a linear constraint on the weights or a quadratic constraint on the weights, respectively. Thus cystic contrast will be improved by using optimal apodization profiles.

The LCLS apodization profiles produce psfs with narrow mainlobes and minimum sidelobe energy. These profiles seem to break the governing rule of windowing in signal processing: in order to achieve lower sidelobes the mainlobe must broaden, a result exhibited by traditional apodization functions. Therefore, the LCLS psfs are more attractive for point imaging in general ultrasound applications, not only imaging anechoic lesions. Although the LCLS design approach improves cystic resolution, it is not truly optimal for imaging diffuse lesions and low echogenicity cysts. In these cases a broader mainlobe may be desirable. Such profiles can be designed using the QCLS approach.

### *B. Enhanced Depth of Field*

The depth of field (DOF) of an ultrasound imaging system is generally defined as the axial region over which the system is in focus, or the axial region over which the system response remains similar to the psf at the focus. Current methods to improve DOF include transmitting at a high f/#, dynamically receiving at low f/#'s, and dynamic receive apodization [41]. The implementation of these techniques lacks formal theory describing effectiveness in improving DOF. Application of the CLS algorithms at every range yields receive weightings that force the psf at each interrogated range to have a specific mainlobe width and the lowest possible sidelobe energy outside that mainlobe. Applying dynamic receive apodization with these weightings will produce similar psfs in range and improve the DOF.

### *C. Optimal Apodization for Harmonic Imaging*

The linear algebra formulation of the psf requires linear superposition on receive but places no linearity constraint on transmit. Conventionally, ultrasound imaging systems assume that the propagation of the sound pulse on transmit is linear and that the receive signal has the same frequency content as that of the transmitted pulse. However, the propagation process is substantially nonlinear and it is possible to receive echoes whose energy content is shifted to harmonics of the fundamental transmit frequency. Imaging with these higher harmonic echoes can improve contrast and resolution in the resulting images. Our CLS techniques can be adapted to calculate receive apodization profiles that take nonlinear propagation into account. The nonlinear propagation of the transmit beam can be determined analytically, experimentally, or through simulation and substituted into the linear algebra formulation of the psf. Assuming linear propagation on receive, the algorithm will design receive aperture functions that minimize the energy of the two-way psf outside a specified boundary. Equation 7 which is rewritten below, describes the relationship between the harmonic imaging scenario and the receive aperture weightings which will minimize the sidelobe energy of the psf. Note that the propagation matrix $S$ will have to take into account the nonlinear propagation effects of the transmit acoustic beam:

$$w_{opt} = (S^T S)^{-1} C [C^T (S^T S)^{-1} C]^{-1} \ .$$

### *D. Arbitrary psf shapes for general imaging, hyperthermia or Doppler applications*

In some scenarios it may be more important to achieve psfs with greater sidelobe rolloff. The weighted CLS formulations described above can achieve such system responses by incorporating

a weight function that increases with distance from the mainlobe. It is also possible with the weighted CLS algorithms to design psfs with localized areas of reduced energy. It should be noted that we focused on producing apodizations that minimized the psf energy in the region lying outside a (typically spherical) void. This procedure was implemented in order to optimize cystic resolution. However, there is no need that the mainlobe and sidelobe regions be delineated according to the shape of a cyst. The CLS formulations can be adapted to design optimal psfs for a variety of ultrasound applications.

In ultrasound hyperthermia procedures, where control of the acoustic energy delivered to the tissue is of great concern [19], designing psfs with multiple mainlobes or "hot spots" while minimizing energy transfer at other locations could improve treatment efficacy as well as shorten treatment times. It is possible with the CLS formulation to specify regions of the psf where delivered energy should be maximized while at the same time specifying regions where acoustic energy should be minimized. In the LCLS design case, the linear constraint could be augmented to constrain the peak gain at a number of point locations, which would result in the $C^T$ vector of (6) becoming a matrix whose row size corresponded to the number of hot spots. The QCLS algorithm may produce even better results for this scenario since the quadratic constraint could be modified to include all regions where the energy of the psf should be constant.

Many authors have considered the issue of improving the estimation of the blood flow velocity vectors by modulating the acoustic beam in the azimuthal direction using the receive apodization function and using an autocorrelation estimator to determine the lateral velocity [42], [43]. Similar CLS formulations could be designed in order to produce apodization profiles that generate psfs with modulation in the azimuthal direction as well as the elevation dimension.

These apodization profiles may be able to produce spatial modulation frequencies higher than those previously produced, reducing the variance of the lateral motion estimates [44].

## DISCUSSION

CLS apodization design is a general formulation for designing mathematically optimal system responses. We describe formulation of this approach for a variety of imaging applications. The required propagation functions can be determined through experiments, simulations, or theory.

Implementing CLS apodization is conceptually and practically simple. Apodization weights could be pre-calculated and stored for the intended application, then retrieved from a look up table during imaging. Current systems already employ dynamic apodization, so implementing the CLS profiles on clinical scanners should be straightforward. However, in order for CLS apodization to be implemented on a clinical system, thorough characterization of the system is required, including the shift variance of the system response. Depending on the system the degree of spatial variance in the impulse response may be great or could be neglected. Either way, once the system has been well characterized our algorithms save a great deal of development time by obviating iterative design.

For cyst imaging, successive imaging with apodization profiles corresponding to all different design cyst radii would be impractical. The question becomes, "which apodization profiles should be used?" Simulation results, presented in an accompanying paper [2], show that CLS apodization profiles are relatively stable across a range of cyst sizes. In fact, profiles calculated for specific cyst radii outperform conventional windows at all cyst sizes. Choosing

the appropriate apodization profile is straightforward when analyzed with the cystic resolution metric. Each apodization yields a contrast curve as a function of cyst radius, and therefore choosing the optimal profile simply requires selecting the apodization that achieves a specified level of contrast for the smallest cyst, or choosing the profile that yields the best contrast for a given cyst size.

The authors acknowledge that the resolution metric, while greatly improving theoretical design considerations, still has some shortcomings. The most worrisome is that the metric describes contrast at a given point in space at a specific instant in time. The metric quantifies contrast of the cyst center versus the background, not the overall cystic contrast. Incorporating detection algorithms, where contrast is defined relative to a speckle region, such as those presented in [45] and [46] may be necessary. This notion raises further questions regarding cyst detectability and observer efficiency [47]. Which cyst is easier to detect: (1) a cyst with well defined boundaries but low overall contrast, or (2) a cyst with blurred edges but greater maximum contrast? A simple one dimensional analysis yields some insights (Fig. 2).

If we view image formation as a simple convolution between the impulse response of the imaging system and the target function, then the CLS algorithms produce two very different results. In one dimension the cyst is modeled as a rect function subtracted from a constant i.e. (1–rect). In the LCLS case, the psf may resemble a triangle function whose base corresponds to the width of the cyst. The resulting image of this cyst will be a smooth Gaussian like function. Note that in Fig. 2 that the resulting convolutions are not to scale with the original inputs. In the QCLS case, the cyst remains the same but the psf resembles a rect function whose width corresponds to the size of the cyst. The resulting image of the cyst will be a triangle function whose negative peak is deeper than that of the smooth Gaussian resulting from the LCLS

apodized psf. It is not obvious which cyst would be more readily detectable. One has sharper edges (LCLS) but the other has a greater maximum contrast. This effect was also seen in Johnson's analysis comparing Hamming and flat apodization [32]. We hope to explore this issue through a human observer study where detection of cysts using the CLS apodization profiles will be investigated.

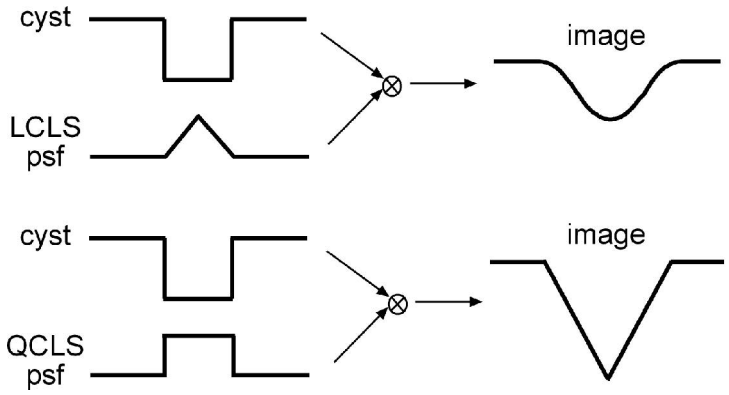


Fig. 2. One dimensional representation of imaging a cyst with the two CLS psfs. In the LCLS case the resulting image of the cyst has sharper defined edges. In the QCLS case the resulting image has blurred edges but more overall contrast than the LCLS imaged cyst.

The design method described here is different than that described in [24] for several reasons. First, we do not require a goal psf in our minimization. Second, our method is considerably easier to implement for broadband imaging systems, while still taking into account the 4 dimensional spatio-temporal nature of the psf. Another difference is that the algorithm described by Ranganathan has no constraints on the design weights which could lead to instability of the results. Our algorithm is similar to the MSSE method described by Ranganathan in that it is general enough to apply to both one way and two way responses, continuous wave and broadband operations, and can be used to design apertures for a variety of

applications. Another similarity is that the entire psf is used to obtain a least squares solution to an overdetermined system of equations.

Our method of apodization profile design for coherent imaging systems is similar to many previously described array pattern synthesis techniques. The LCLS formulation is similar to the array pattern synthesis technique by Tseng [8], however we use a broadband formulation, a different linear constraint on the weights, and our algorithm does not require iterations to achieve an optimum. This QCLS formulation is similar to the constrained eigenfilter design [10], [26]; however, we use a broadband formulation and a quadratic constraint on the energy in the psf.

Keitmann-Curdes *et al.* [27] used a formulation similar to our QCLS formulation in designing optimal apodizations in simulated ultrasound fields. However, their method minimized the energy in the sidelobes of the system response over time. The use of space-time psfs in their model neglects the inherent shift variant properties of the imaging system and integrating the pressure field power over the time axis is not a realistic measure of the system's spatial impulse response. Finally Schwann *et al.* elegantly used two different resolution criteria to design frequency dependent receive apodization profiles [28]. Their resolution criteria: maximum to average ratio and the fill-in measure relate directly to cystic contrast. However, their multiple objective formulation requires computationally expensive iterative methods to arrive at one Pareto optimum solution. Furthermore, given a Pareto optimal frontier, a curve of all the Pareto optimal solutions as a function of the objectives, for the maximum to average ratio versus fill-in criteria, it is unclear as to what point on that curve is truly optimal for clinical ultrasound imaging. The contrast curves we produce using the cystic resolution metric on the other hand, provide a straightforward approach for parameter optimization.

Our method offers an elegant path for optimizing the ultrasound system's psf and has potential application to apodization design for many varied applications. Overall, the CLS apodization design technique has the potential to improve the contrast of anechoic legions and improve beamforming in general by forming psfs with narrow mainlobes and low sidelobes. The technique may also aid in the design of system responses used for hyperthermia applications and Doppler signal processing. Stability of the CLS algorithms in the presence of sound speed errors as well as changing system parameters needs to be investigated. Simulation results addressing these issues for the CLS apodization design technique and its applications are described in an accompanying paper [2]. Results show that CLS apodization profiles improve cystic contrast compared to many conventional windows as well as improve DOF.

**Conclusion**

The CLS apodization design technique presented in this paper is a general beamforming method that can be used to design apertures for specific applications. It achieves mathematically optimal cystic contrast by designing mathematically optimal aperture weights for a given system. The contrast is optimized because the weights minimize the energy of the psf outside the specified cyst boundary while either maintaining peak gain inside the cyst (LCLS) or maintaining constant psf energy inside the cyst (QCLS). The CLS apodization design technique also has the potential to improve point resolution by forming psfs that have narrower mainlobes and lower sidelobes than psfs generated from conventional windows. Therefore, we believe the CLS apodization design algorithms have significant potential to improve ultrasound beamforming and can be applied in any ultrasound application where the system response is well characterized.

## REFERENCES


[1] K. Ranganthan and W. F. Walker, "A General Cystic Resolution Metric for Medical Ultrasound," submitted to the *IEEE Transactions on Ultrasonics, Ferroelectrics, and Frequency Control*.

[2] D. A. Guenther and W. F. Walker, "Optimal Apodization Design for Medical Ultrasound using Constrained Least Squares. Part II: Simulation Results," submitted to the *IEEE Transactions on Ultrasonics, Ferroelectrics, and Frequency Control*.

[3] C. L. Dolph, "A current distribution for broadside arrays which optimizes the relationship between beamwidth and sidelobe level," *Proc. IRE*, vol. 34, pp. 335-348, 1946.

[4] T. T. Taylor, "Design of line source antennas for narrow beamwidth and low sidelobes," *IRE Trans. Antennas Propagat.*, vol. AP-3, pp. 16-28, 1955.

[5] A. T. Villeneuve, "Taylor Patterns for Discrete Arrays," *IEEE Trans. Antennas Propagat.*, vol. 32, no. 10, pp 1089-1093, 1984.

[6] A. H. Nuttall, "Some Windows with Very Good Sidelobe Behavior." *IEEE Trans. Acoust. Speech Signal Process.*, vol. 29, no. 1, pp. 84-91, 1981.

[7] C. A. Olen and R. T. Compton, Jr., "A Numerical Pattern Synthesis Algorithm for Arrays," *IEEE Trans. Antennas Propagat*., vol. 38, no. 10, pp. 1666-1676, 1990.

[8] C.-Y Tseng and L. J. Griffiths, "A Simple Algorithm to Achieve Desired Patterns for Arbitrary Arrays," *IEEE Trans. Signal Proc*., vol. 40, no. 11, pp. 2737-2746, 1992.

[9] I. W. Selesnick, M. Lang, and C. S. Burrus, "Constrained Least Square Design of FIR Filters without Specified Transition Bands," *IEEE Trans. Signal Proc*., vol. 44, no.8, pp. 1879-1892, 1996.

[10] Y.-M. Law and C.-W. Kok, "Constrained Eigenfilter Design Without Specified Transition Bands," *IEEE Trans. On Circuits and Systems-II: Express Briefs*, vol. 52, no. 1, pp. 14-21, 2005.

[11] S.-C. Pei and J.-J. Shyu, "2-D FIR Eigenfilters: A Least-Squares Approach," *IEEE Trans. Circuits and Systems*, vol. 37, no. 1, pp. 24-43, 1990.

[12] P. P. Vaidyanathan and T. Q. Nguyen, "Eigenfilters: A New Approach to Least-Squares FIR Filter Design and Applications Including Nyquist Filters," *IEEE Trans. Circuits and Systems*, vol. 34, no. 1, pp. 11-23, 1987.

[13] M. H. Er, "Array Pattern Synthesis with a Controlled Meas-Square Sidelobe Level," *IEEE Trans. Signal Proc*., vol. 40, no. 4, pp. 977-981, 1992.

[14] S. L. Sim and M. H. Er, "Constrained optimization technique for general array pattern synthesis," *Electronics Letters*, vol. 32, no. 10, pp. 861-862, 1996.

[15] M. H. Er, S. L. Sim, and S. N. Koh, "Application of constrained optimization techniques to array pattern synthesis," *Signal Processing*, vol. 34, pp. 323-334, 1993.

[16] M. H. Er, "On the Limiting Solution of Quadratically Constrained Broad-Band Beam Formers," *IEEE Trans. Signal Proc*., vol. 41, no. 1, pp. 418-419, 1993.

[17] S. L. Sim and M. H. Er, "Sidelobe suppression for general arrays in presence of element failures," *Electronics Letters*, vol. 33, no. 15, pp. 1278-1280, 1997.

[18] B.P. Ng, M. H. Er, and C. Kot, "Linear array geometry synthesis with minimum sidelobe level and null control," *IEE Proc. Microw. Antennas Propagat*., vol. 141, no. 3, pp. 162-166, 1994.

[19] E. S. Ebbini and C. Cain, "Multiple-focus ultrasound phased-array pattern synthesis: Optimal driving-signal distributions for hyperthermia," *IEEE Trans. Ultrason. Ferroelect.,and Freq. Contr*., vol. 36, no. 5, pp. 540-548, 1989.

[20] P.-C. Li, S. W. Flax, E. S. Ebbini, and M. O'Donnell, "Blocked element compensation in phased array imaging*," IEEE Trans. Ultrason. Ferroelect., and Freq. Contr*., vol. 40, no. 4, pp. 283-292, 1993.

[21] B. Mandersson and G. Salomonsson, "Weighted Least-Squares Pulse-Shaping Filters with Application to Ultrasonic Signals," *IEEE Trans. Ultrason. Ferroelect., and Freq. Contr*., vol. 36, no. 1, pp. 109-113, 1989.

[22] W. Wilkening, B. Brendel, H. Jiang, J. Lazenby, and H. Ermert, "Optimized Receive Filters and Phase-Coded Pulse Sequences for Contrast Agent and Nonlinear Imaging," *Proc. IEEE Ultrason. Symp*., pp. 1733-1737, 2001.

[23] W. Wilkening, B. Brendel, C. Hansen, and H. Ermert, "Optimized Filters for Dynamic RF Echo Blending in Multiple Focal Zone Imaging," *Proc. IEEE Ultrason. Symp*., pp. 1729-1732, 2004.

[24] K. Ranganathan and W. F. Walker, "A novel beamformer design method for medical ultrasound. Part I: Theory*," IEEE Trans. Ultrason., Ferroelect., and Freq. Contr*., vol. 50, no. 1, pp. 15-24, 2003.

[25] K. Ranganathan and W. F. Walker, "A novel beamformer design method for medical ultrasound. Part II: Results," *IEEE Trans. Ultrason., Ferroelect., and Freq. Contr*., vol. 50, no. 1, pp. 25-39, 2003.

[26] S. Docolo and M. Moonen, "Design of far-field and near-field broadband beamformers using eigenfilters," *Signal Processing*, vol. 83, pp. 2641-2673, 2003.

[27] O. Keitmann-Curdes, B. Brendel, C. Marg, and H. Ermert, "Optimization of Apodization Based on the Sidelobe Pressure Energy in Simulated Ultrasound Fields," *Proc. IEEE Ultrason. Symp*., pp. 1677-1680, 2002.

[28] R. Schwann, N. Stache, and T. G. Noll, "Optimization of Frequency Dependent Receive Apodization," presented at the *2005 IEEE International Ultrasonics Symposium*, 18-21 Sept. 2005, Rotterdam, The Netherlands. In press.

[29] M. D. Intriligator, *Mathematical Optimization and Economic Theory*. Pennsylvania: Society for Industrial and Applied Mathematics, 2002, p. 258.

[30] B. D. Steinberg, *Principles of Aperture and Array System Design*, John Wiley & Sons, 1976, pp. 40-52.

[31] D. Vilkomerson, J. Greenleaf, and V. Dutt, "Towards a resolution metric for medical ultrasonic imaging," *Proc. IEEE Ultrason. Symp*., vol. 2, pp. 1405-1410, 1995.

[32] R. Johnson, "Contrast Response Analysis for Medical Ultrasound Imaging," *IEEE Trans. Ultrason., Ferroelect., and Freq. Contr*., vol. 44, no. 4, pp. 805-809, 1997.

[33] K. F. Üstüner and G. L. Holley, "Ultrasound Imaging System Performance Assessment," presented at the *2003 AAPM Annual Meeting*.

[34] J. W. Goodman, *Introduction to Fourier Optics, 3rd ed*. Colorado: Roberts & Company, 2005.

[35] A. R. Selfridge, G. S. Kino, and B. T. Khuri-Yakub, "A theory for the radiation pattern of a narrow-strip acoustic transducer," Appl. Phys. Lett., vol. 37, no. 1, pp.35-36, 1980.

[36] L. L. Scharf, Statistical Signal Processing: Detection, Estimation, and Time Series Analysis, Addison-Wesley Publishing Company, 1991, p.365.

[37] Y. Y. Haimes, *Risk Modeling, Assessment, and Management, 2nd ed.* John Wiley and Sons, Inc., 2004.

[38] G. H. Golub and C. F. Van Loan, *Matrix Computations, 3rd ed.* Baltimore: The Johns Hopkins University Press, pp. 375-378, 1996.

[39] W. H. Gander, "Least Squares with a Quadratic Constraint," Numerische Mathematik, vol. 36, pp. 291-307, 1981.

[40] A. Björck, *Numerical Methods for Least Squares Problems*. Philadelphia, Society for Industrial and Applied Mathematics, pp. 203-213, 1996.

[41] K. Thomenius, "Evolution of ultrasound beamformers," in Proc. IEEE Ultrason. Symp., 1996, pp. 1615-1622.

[42] J. A. Jensen and P. Munk, "A new method for estimation of velocity vectors," *IEEE Trans. Ultrason., Ferroelect., and Freq. Contr.,* vol. 45, pp. 837-851, 1998.

[43] M. E. Anderson, "Spatial Quadrature: A novel technique for multidimensional velocity estimation," In *Proc. IEEE Ultrason. Symp.*, vol. 45, pp. 1233-1238, 1997.

[44] W. F. Walker and G. E. Trahey, "A Fundamental Limit on Delay Estimation Using Partially Correlated Speckle Signals," *IEEE Trans. Ultrason., Ferroelect., and Freq. Contr.,* vol. 42, pp. 301-308, 1995.

[45] S. W. Smith, R. F. Wagner, J. M. Sandrik, and H. Lopez, "Low Contrast Detectability and Contrast/Detail Analysis in Medical Ultrasound," *IEEE Trans. Sonics and Ultrason*., vol. 30, no. 3, pp. 164-173, 1983.

[46] S. W. Smith and H. Lopez, "A contrast-detail analysis of diagnostic ultrasound imaging," *Med. Phys.*, vol. 9, no. 1, pp. 4-12, 1982.

[47] C. K. Abbey, R. J. Zemp, J. Liu, K. K. Lindfors, and M. F. Insana, "Observer Efficiency in Discrimination Tasks Simulating Malignant and Benign Breast Lesions Imaged With Ultrasound," *IEEE Trans. Medical Imaging*, vol. 25, no. 2, pp. 198-209, 2006.